Galaxy formation at high redshifts

N. Metcalfe, T. Shanks, A. Campos*, R. Fong & J. P. Gardner

Physics Department, University of Durham, South Road, Durham DH1 3LE, UK
* Present address: Instituto de Astrofisica de Andalucia, CSIC, Spain.

Sensitive optical surveys have revealed[1] a large population of 'faint blue galaxies', which are believed to be young galaxies observed close to their time of formation[2]. But there has been considerable uncertainty regarding the epochs at which these galaxies are observed, owing to the difficulties inherent in determining spectroscopic redshifts for very faint objects. Here, by modelling the numbers and colours of galaxies at the faintest detection limits, we show that the faint blue galaxies are likely to lie at high redshift ($z \approx 2$). This conclusion holds regardless of whether the Universe is assumed to be open or at the critical density (flat). In an open universe, the data are consistent with galaxy models in which star formation rates decay exponentially with decreasing redshift, whereas the assumption of a flat universe requires the addition of a population of galaxies which are seen only at high redshift.

We have measured galaxy counts and colours in the Deep Field[3] recently observed by the Hubble Space Telescope (HST) to $U = 27$ mag, $B = 29$ mag, $R = 28.5$ mag and $I = 28$ mag. The HST data covers 5.3 arcmin^2 and the exposure times were ~25 h in each of the BRI bands and ~47 h in the U band. Similar techniques, adjusted for the smaller image size, were used to analyse the HST data as we have previously used to analyse deep ground-based images[4,5]. Taking these deepest galaxy count data together with the results of recent galaxy redshift surveys at the spectroscopic limit of the Keck Telescope[6,7], reveals the clearest picture so far of the Universe at faint magnitudes.

The derived HST B galaxy number counts are shown in Fig. 1, together with those from other work, including the deepest ground-based counts from the William Herschel Telescope (WHT) to $B = 28.2$ mag. The HST and WHT results are seen to be in good agreement to this limit, with the HST counts extending ~1 mag fainter. Figure 1 also shows the HST counts in the I band. In this band the HST data extends about ten times deeper than previous data, because of the higher HST resolution and the fainter background sky. Although HST has as yet no K-band imaging capability, we also summarise in Fig. 1 the deepest ground-based K counts, including new data from the UK Infrared Telescope (UKIRT). The K counts now appear to be reasonably well defined in the range 13 mag $< K <$ 24 mag.

We first compare the count data with non-evolving models. In the modelling we assume throughout a Hubble constant of $H_0 = 50\,\mathrm{km\,s^{-1}\,M\,pc^{-1}}$, but our main conclusions below are insensitive to this assumption. As can be seen from Fig. 1, the non-evolving models increasingly underestimate the optical counts at faint magnitudes. However, as noted previously, the magnitude at which the 'faint blue galaxy' excess becomes apparent is dependent on the normalization of the models at bright magnitudes. With the high normalization adopted here, non-evolving models give a reasonable representation of the bright counts and redshift distributions in the range 18 mag $< B <$ 22.5 mag (refs 1, 4, 5, 8, 9)

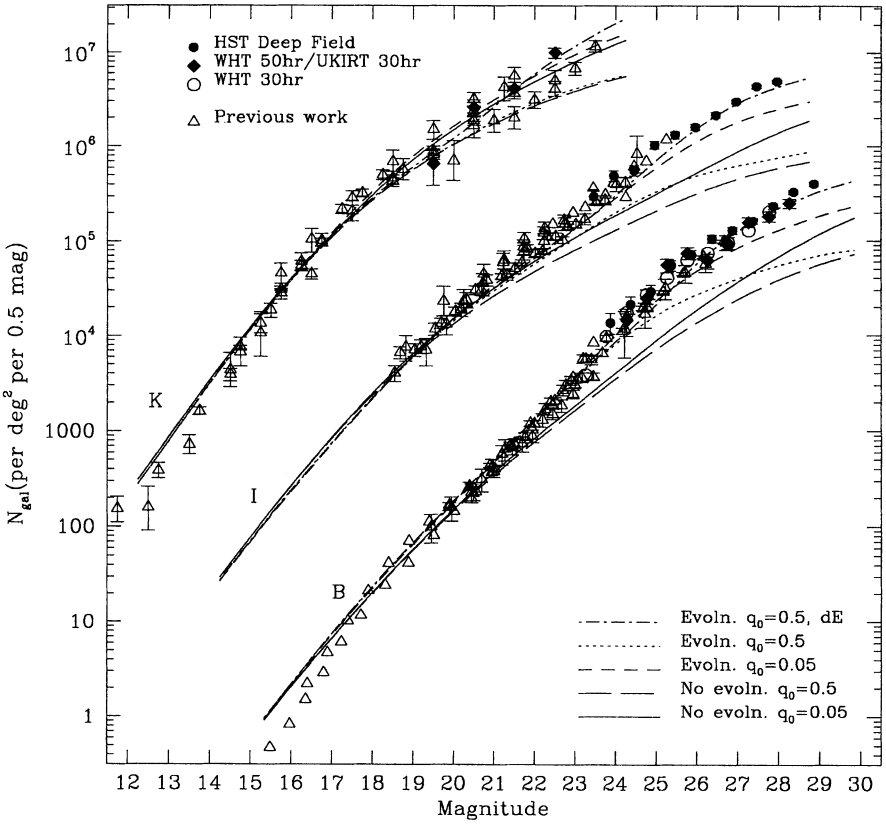

FIG. 1 The B (Johnson) and I (Kron–Cousins) galaxy counts from the HST Deep Field (F450W, F814W) data compared to counts from the WHT, UKIRT and elsewhere (refs 1, 4, 5, 10, 11, 22–29). Also shown are deep K-band galaxy counts from ground-based data. The I-band counts have been multiplied by a factor of 10, and the K-band counts have been multiplied by a factor of 100, for clarity. (The HST U and R counts are available: see Supplementary Information.) The model luminosity function parameters and other details of the modelling procedure are given elsewhere[4,5]. The galaxy luminosity evolution with redshift is computed from Bruzual and Charlot[12] isochrone synthesis models, using the appropriate passbands. We assume galaxy ages of 16 and 12.7 Gyr in the cases $q_0 = 0.05$, 0.5. We adopt a dwarf-dominated IMF ($x = 3$) with an exponentially increasing star-formation rate of timescale, $\tau = 2.5$ Gyr, for E/SO/Sab galaxies, and a Salpeter IMF ($x = 1.35$) with an exponentially increasing star-formation rate of time scale, $\tau = 9$ Gyr, for Sbc/Scd/Sdm galaxies. The latter are also assumed to have internal dust absorption at $z = 0$ of $A_B = 0.3$ mag, $A_I = 0.11$ mag, $A_K = 0.03$ mag. We take an absorption law inversely proportional to the wavelength λ, $A_\lambda \propto 1/\lambda$, to approximate the effect of redshift on the internal dust absorption. The models also include the effect of Lyman-α forest/break absorption[21]. Spiral evolution dominates these models in the B and I bands. The $q_0 = 0.05$ evolving model gives a good fit to $B \approx 27$ mag, $I \approx 26$ mag, whereas the $q_0 = 0.5$ model only fits to $B \approx 25$ mag, $I \approx 23.5$ mag. The fit of the $q_0 = 0.5$ model is improved when an extra high redshift galaxy population (dE) with constant star formation rate (SFR) at $z > 1$ and rapidly fading at $z < 1$ is invoked. The Schechter luminosity function parameters of the dE population at $z = 0$ are $M_B^* = -16.0$ mag, $\alpha = -1.2$ and $\phi^* = 0.019\,\mathrm{mag^{-1}\,Mpc^{-3}}$. The K galaxy counts, in contrast to the B and I counts, are well fitted by non-evolving models.

and also to individual counts of spiral and early-type galaxies at similar magnitudes[10,11]. As a consequence, the B galaxy count then only shows evidence for strong evolution in the range $B > 23$ mag. Also the high normalization allows non-evolving models with deceleration parameter, $0.05 < q_0 < 0.5$ to fit the K counts from $K = 15$ mag to the faintest count limit at $K = 24$ mag. This is as expected, since evolved, young star populations are expected to affect galaxy light less in the infrared than in the blue.

To fit the optical counts, we then consider simple evolutionary models from Bruzual and Charlot[12] where galaxy star-formation rates rise exponentially with look-back time. In such models, the galaxy light at early times is generally dominated by luminous, blue stars but at later times, when these stars fade and the star-formation rate slows, the galaxy light dims and reddens. These models are known to fit the B counts in the range $18\,\text{mag} < B < 25\,\text{mag}$[1,4,5,8,9]. But previous faint galaxy redshift surveys at $B < 24$ mag presented a problem for such models, as they predict a high-redshift tail of evolved, luminous galaxies which was unobserved in these surveys[13]. However, these surveys were frequently only ~60% complete, and the galaxies with unidentified redshifts were usually blue. Recently Cowie *et al.*[6,7] have used the Keck 10-m telescope to make a new $B < 24$ mag galaxy redshift survey with >80% completeness and have detected such a high-redshift galaxy component, supporting the basic viability of these models (see Fig. 2). An extended high-redshift tail is also consistent with the low galaxy clustering amplitude observed[9] at $B > 23$ mag.

A further new development is that the latest version of the preferred spiral galaxy evolution model[12] now permits more brightening at high redshift, while still reproducing the blue colours of spirals at the present day[14]. Combined with the steep luminosity function of spirals[8] and assuming a small amount of internal dust[14–16], this enables us to obtain a good fit to the high-redshift tail of the Keck number–redshift distribution, $n(z)$, at $22.5\,\text{mag} < B < 24\,\text{mag}$ (see Fig. 2) and to other redshift survey results[17]. In the low-q_0 case, this spiral-dominated model then also produces a reasonable fit to the optical counts to $B \approx 27$ mag and $I \approx 26$ mag (see Fig. 1). Although the model underestimates the optical counts at fainter magnitudes, this discrepancy is probably still within the combined data and model uncertainties. In the $q_0 = 0.5$ case, the spiral luminosity evolution model only fits the optical data to $B \approx 25$ mag and $I \approx 23.5$ mag and then more seriously underestimates the counts at fainter magnitudes. Thus, the HST data confirms the previous

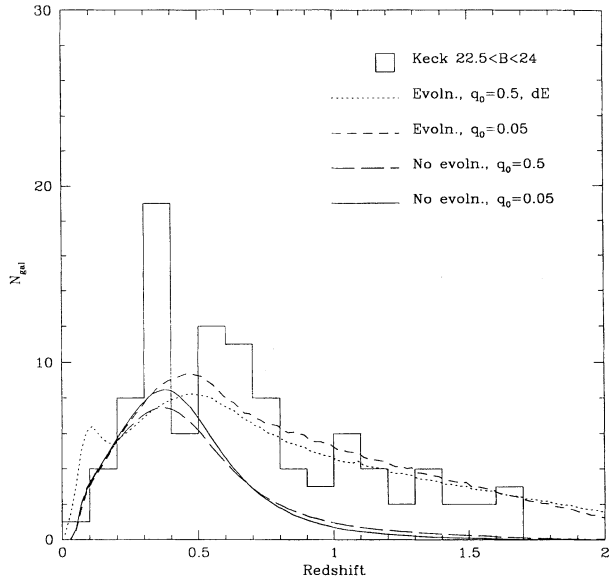

FIG. 2 The galaxy number–redshift distribution, $n(z)$, for $22.5\,\text{mag} < B < 24$ mag implied by new redshift data acquired on the Keck Telescope (refs. 6, 7). The observed $n(z)$ is clearly more extended than the non-evolving models with either $q_0 = 0.05$ or $q_0 = 0.5$. The extended redshift distribution is well fitted by our evolutionary models whose parameters are described in Fig. 1 legend.

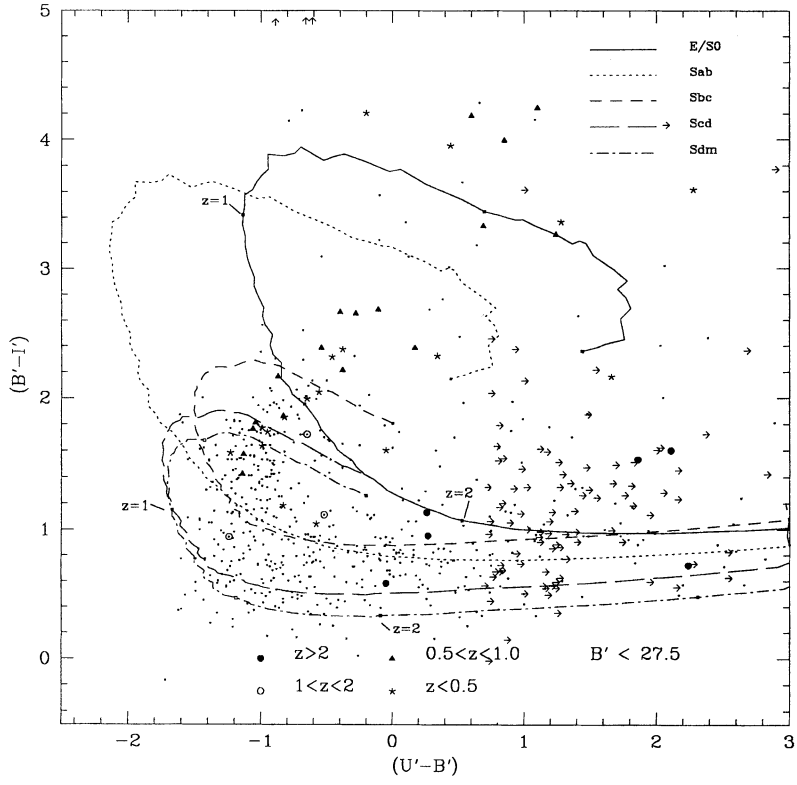

FIG. 3 Dots represent the $U' - B' : B' - I'$ colours of galaxies with $B' < 27.5$ mag in the Hubble Deep Field. Primed letters for magnitudes indicate that here we are using the natural HST magnitude system, with the zero point set at an A0V star. The arrows represent detection upper limits, mainly galaxies which are undetected in U'. The $U' - B'$ colours move sharply redwards at $B' - I' \approx 0.8$ due to the Lyman-α forest/Lyman break passing through the U' band. The predicted tracks are the $q_0 = 0.05$ evolutionary models for each morphological type as detailed in Fig. 1 legend, modulated in the case of Sbc/Scd/Sdm types by our assumed internal dust absorption of $A'_U = 0.45$ mag, $A'_B = 0.3$ mag, $A'_I = 0.11$ mag and in the case of all galaxies by the Lyman-α forest absorption. The models used in the $q_0 = 0.5$ case (not shown) show a very similar behaviour, even for the rapidly fading dE type. The $z = 1$ and $z = 2$ labelled positions on the tracks indicate the colours of model E/SO and Sdm galaxies at these redshifts. The remaining symbols show the colours of 45 brighter galaxies with Keck spectroscopic redshifts, and these agree well with the predicted colours for these galaxies. It can also be seen that $U' - B' < 0$ is predicted to correspond to galaxies with $z < 2$, and $U' - B' > 0$ to galaxies with $z > 2$.

ground-based result[1,4,5,18] that if $q_0 = 0.5$, then there is not enough spatial volume at high redshifts to allow simple luminosity evolution models to fit the high galaxy counts at $B > 25$ mag. This confirmation is important because confusion corrections are much smaller in the high-resolution HST galaxy counts than in previous ground-based data.

We have already noted that the faint K counts seem less affected by evolution and this is supported by the new Keck redshift data[6,7], where non-evolving models again give a good fit to the $n(z)$ relation for 18 mag $< K <$ 19 mag (ref. 7). As non-evolving models imply that, at $K < 20$ mag, the majority of galaxies are early types, this suggests that early-type galaxies may be little affected by either dynamical (merging) or luminosity evolution. Indeed, although the effect of passive evolution of early-type galaxies with a Salpeter initial mass function (IMF) slope ($x = 1.35$) is small at K (<0.7 mag at $z = 1$), it is still big enough to make the predicted Keck $n(z)$ appear too extended at 18 mag $< K <$ 19 mag (refs 6, 7). If the result is not due to incompleteness, then the amount of K evolution can be reduced to acceptable limits by assuming a more dwarf-dominated IMF ($x = 3$) for early-type galaxies. While awaiting more complete K surveys, we have adopted this dwarf-dominated IMF for early types throughout this paper.

To improve the fit of the $q_0 = 0.5$ model to the faint optical counts, we consider a model with an extra population of high-redshift galaxies which have a constant star-formation rate from the formation epoch till $z = 1$ (~4 Gyr after formation with our assumed H_0). The Bruzual and Charlot[12] model shows that at $z \lesssim 1$ the galaxy then rapidly fades by 5 magnitudes in B to form a red (dE) galaxy by the present day. This model is in the spirit of previously proposed 'disappearing dwarf' count models[19] and it gives a good fit to the faint B, I and K counts and the Keck $n(z)$ data (see Figs 1 and 2).

We next test these models against the faint galaxy colour distributions in the Hubble Deep Field. The presence of broad features in galaxy spectra allows tests to be made of the predicted galaxy redshifts. One approach is to use the HST broad-band photometry as a rough galaxy spectrum and then derive redshifts for individual galaxies using local galaxies as templates[20]. Here we follow the different approach of simply comparing our evolutionary model predictions to the observations of faint galaxy colours. We see in Fig. 3 that our predicted $U' - B' : B' - I'$ model tracks, that is, the loci traced by model galaxy colours as they change with redshift, compare well with the observed colours for $B' < 27.5$ mag galaxies. (Primed letters here denote the natural HST magnitude system). In particular, the redshifting of the

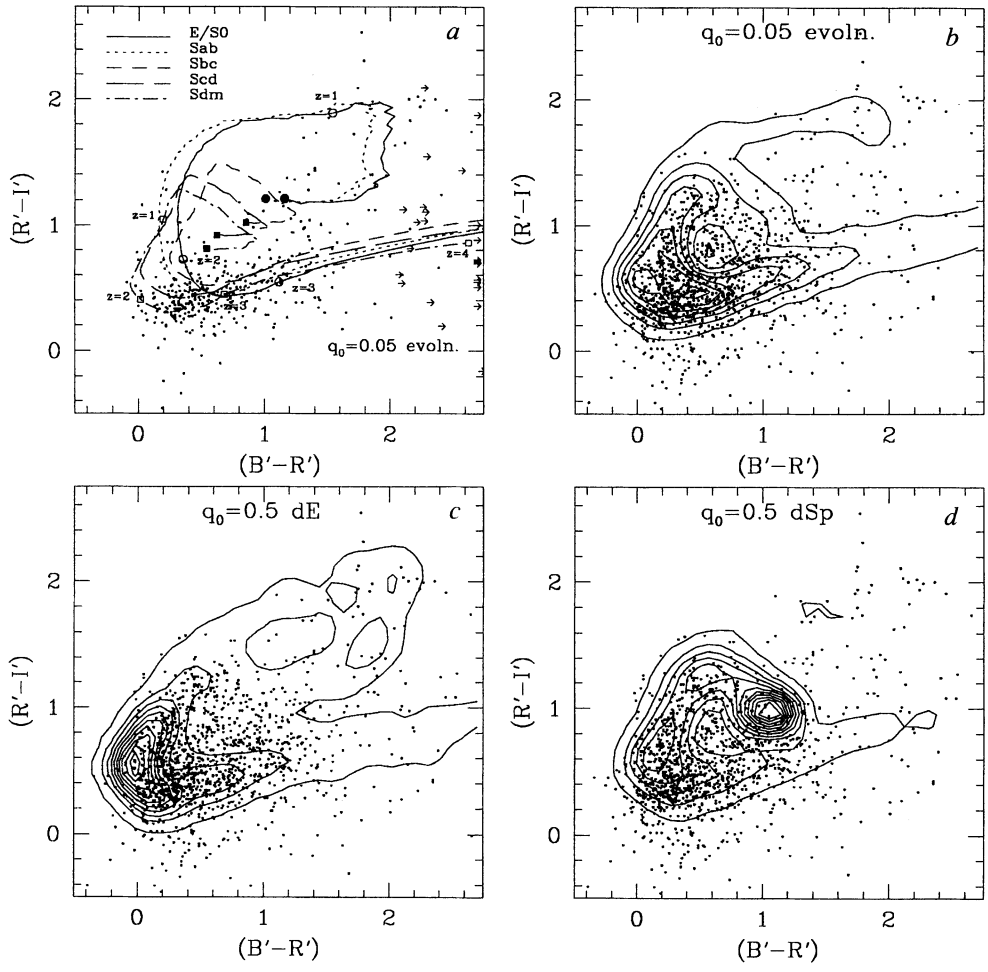

FIG. 4*a*, The $q_0 = 0.05$ evolutionary models' $B' - R' : R' - I'$ tracks with redshift, as a function of galaxy morphological type. Primed letters for magnitudes indicate that here we are using the natural HST magnitude system, zero-pointed to an A0V star. The tracks are modulated by our assumed internal dust and Lyman-α forest/break absorption. A filled symbol marks each galaxy type's colour at zero redshift. The open symbols mark the galaxy type's colour at unit intervals in redshift for E/S0 and Sdm galaxies. Galaxies with $B' - R' = 0.3$ mag and $R' - I' = 0.6$ mag have $z \approx 2$. The same is true for the $q_0 = 0.5$ models, even for the rapidly fading dE type (not shown). The dots indicate the colours of galaxies with $R' < 27.5$ mag and $U' - B' > 0$ which are predicted to have $z > 2$. Their position in the independent $B' - R' : R' - I'$ plane is consistent with this prediction. *b*, Dots represent the $B' - R' : R' - I'$ colours of $R' < 28$ mag galaxies in the Hubble Deep Field. These show the same horse-shoe-shaped track as expected from the models in *a*. The contours represent the relative numbers of galaxies predicted for the $q_0 = 0.05$ evolutionary model, which appear to be in good agreement with the data, peaking at the colours corresponding to $z \approx 2$. *c*, As *b*, but with the contours here representing the relative numbers of galaxies predicted for the $q_0 = 0.5$ 'disappearing dwarf' (dE) model, which again appear to be in reasonable agreement with the data. *d*, As *b* but with the contours here representing the relative numbers of galaxies predicted for the $q_0 = 0.5$ low-redshift dwarf (dSp) model. The data show that this model is inappropriate, as it clearly predicts too many low-redshift, $z \approx 0.5$, spiral galaxies.

Lyman-α forest/break[21] absorption features through the U' band causes the model $U'-B'$ colours to move sharply redwards at $B'-I' \approx 0.7$ mag and the same effect is clearly seen in the data. The colours of 45 brighter, $B \approx 24$ mag galaxies with Keck redshifts are also shown in Fig. 3, and are also found to agree well with their predicted colours. (The equivalent $B'-R'$ versus $R'-I'$ graph is available: see Supplementary Information).

The above predictions show that, for the majority of faint galaxies, $U'-B' < 0$ is predicted to correspond to $z < 2$ galaxies and $U'-B' > 0$ corresponds to $z > 2$ galaxies. We find that the proportion of galaxies with $U'-B' > 0$ (including those undetected in U') rises to $47 \pm 7\%$ of the total at 27 mag $< B <$ 28 mag, indicating that the redshift distribution may peak at $z \approx 2$. This fraction is matched very well by both the $q_0 = 0.05$ model which predicts 47% with $U'-B' > 0$ at the same limit and the $q_0 = 0.5$, disappearing dwarf (dE) model which predicts 43%. We have also considered another $q_0 = 0.5$ model which assumes an extra population of low-redshift dwarf spirals (dSp) which evolve more slowly according to our standard exponential model for spiral luminosity evolution[12]. Although this model also gives an improved fit to the counts, it predicts too few high-redshift ($U'-B' > 0$) galaxies (28%) for compatibility with the faint HST data.

These conclusions are confirmed by consideration of the $B'-R'$ versus $R'-I'$ colour–colour plot in Fig. 4. Figure 4*a* shows the predicted tracks of the galaxy types with redshift, as in Fig. 3. Also plotted are the galaxies with $U'-B' > 0$ and $R' < 27.5$ mag; these are expected to have $z > 2$ by the above arguments and it can be seen that their position on the $B'-R' : R'-I'$ tracks is entirely consistent with their lying in this redshift range. We regard this as crucial confirmation that our models are indicating consistent redshifts for galaxies in $U'-B'$ and $B'-R' : R'-I'$ independently. Figure 4*b*, *c*, *d* then show the HST data (dots) at $R' < 28$ mag compared to the predicted galaxy number contours for the open and closed models, based on the tracks shown in Fig. 4*a*. Both the $q_0 = 0.05$ and the $q_0 = 0.05$ dE model contours give a reasonable fit to the data which seem to peak at $B'-R' \approx 0.3$, $R'-I' \approx 0.3$, corresponding to $z \approx 2$ for all galaxy types. However, the $q_0 = 0.05$ dSp model contours peak away from this point at $B'-R' \approx 1$, $R'-I' \approx 1$ which corresponds to $z \approx 0.5$ for the dwarf spiral galaxies and we conclude that the galaxy redshift distribution in this model is skewed to too low redshifts to be compatible with the colour data. This does not mean that the above 'disappearing dwarf' model is unique in allowing a fit to be obtained with $q_0 = 0.5$; other possibilities such as merging models may also exist. However, it does suggest that, in any model, the star-forming phase has to be at $z \approx 2$ for consistency with the faint galaxy colours in the Hubble Deep Field. □

Received 12 February; accepted 13 August 1996.

1. Koo, D. C. & Kron, R. G. *Ann. Rev. Astron. Astrophys.* **30,** 613–652 (1992).
2. Cowie, L. L. in *The Post-Recombination Universe* (eds Kaiser, N. & Lasenby, A.) 1–18 (Kluwer, Dordrecht, 1990).
3. Williams, R. E. *et al. Astron. J.* (in the press).
4. Metcalfe, N., Shanks, T., Fong, R. & Jones, L. R. *Mon. Not. R. Astron. aSco.* **249,** 481–497 (1991).
5. Metcalfe, N., Shanks, T., Fong, R. & Roche, N. *Mon. Not. R. Astron. Soc.* **273,** 257–276 (1995).
6. Cowie, L. L., Hu, E. M. & Songaila, A. *Nature* **377,** 603–605 (1995).
7. Cowie, L. L., Songaila, A., Hu, E. M. & Cohen, J. G. *Astron. J.* (in the press).
8. Shanks, T. in *The Galactic and Extragalactic Background Radiations* (eds Bowyer, S. & Leinert, C.) 269–281 (Kluwer, Dordrecht, 1990).
9. Roche, N., Shanks, T., Metcalfe, N. & Fong, R. *Mon. Not. R. Astron. Soc.* **263,** 360–368 (1993).
10. Glazebrook, K., Ellis, R. S., Santiago, B. & Griffiths, R. *Mon. Not. R. Astron. Soc.* **275,** L19–L22 (1995).
11. Driver, S. P. *et al. Astrophys. J.* **449,** L23–L28 (1995).
12. Bruzual, A. G. & Charlot, S. *Astrophys. J.* **405,** 538–553 (1993).
13. Glazebrook, K. *et al. Mon. Not. R. Astron. Soc.* **273,** 157–168 (1995).
14. Campos, A. & Shanks, T. *Mon. Not. R. Astron. Soc.* (submitted).
15. Wang, B. *Astrophys. J.* **383,** L37–L40 (1991).
16. Gronwall, C. & Koo, D. C. *Astrophys. J.* **440,** L1–L4 (1995).
17. Lilly, S. J., Tresse, L., Hammer, F., Crampton, D. & Le Febre, O. *Astrophys. J.* **455,** 108–124 (1995).
18. Yoshii, Y. & Takahara, F. *Astrophys. J.* **326,** 1–18 (1988).
19. Babul, A. & Rees, M. J. *Mon. Not. R. Astron. Soc.* **255,** 346–350 (1992).
20. Lanzetta, K. M., Yahil, A. & Fernandex-Soto, A. *Nature* **381,** 759–763 (1996).
21. Madau, P. *Astrophys. J.* **441,** 18–27 (1995).
22. Smail, I., Hogg, D. W., Yan, L. & Cohen, J. G. *Mon. Not. R. Astron. Soc.* (in the press).
23. Driver, S. P., Phillipps, S., Davies, J. I., Morgan, I. & Disney, M. J. *Mon. Not. R. Astron. Soc.* **268,** 393–404 (1994).
24. Djorgovski, S. *et al. Astrophys. J.* **438,** L13–L16 (1995).
25. Gardner, J. P., Cowie, L. L. & Wainscoat, R. J. *Astrophys. J.* **415,** L9–L12 (1993).
26. Soifer, B. T. *et al. Astrophys. J.* **420,** L1–L4 (1994).
27. McLeod, B. A., Bernstein, G. M., Rieke, M. J., Tollestrup, E. V. & Fazio, G. G. *Astrophys. J. Suppl. Ser.* **96,** 117–121 (1995).
28. Glazebrook, K., Peacock, J. A., Collins, C. A. & Miller, L. *Mon. Not. R. Astron. Soc.* **266,** 65–91 (1995).
29. Gardner, J. P., Sharples, R. M., Carrasco, B. E. & Frenk, C. S. *Mon. Not. R. Astron. Soc.* (submitted).

SUPPLEMENTARY INFORMATION. Available on *Nature*'s World-Wide Web site http://www.nature.com or as paper copies form Mary Sheehan at the London editorial office of *Nature*.

ACKNOWLEDGEMENTS. We thank L. L. Cowie for allowing us to use results from the Keck 10-m redshift surveys in advance of publication, A. G. Bruzual for producing dwarf-dominated evolutionary models specially for this Letter, and the referees for helpful comments. We acknowledge the use of the Hubble Space Telescope Deep Field data. A.C. was supported by an EC Fellowship, and N.M. and J.P.G. by the UK PPARC.

CORRESPONDENCE should be addressed to T.S. (e-mail: Tom.Shanks@durham.ac.uk).

Entropic control of particle motion using passive surface microstructures

A. D. Dinsmore*, A. G. Yodh* & D. J. Pine†

* Department of Physics and Astronomy, University of Pennsylvania, 209 South 33 Street, Philadelphia, Pennsylvania 19104, USA
† Departments of Chemical Engineering and Materials, University of California, Santa Barbara, California 93106, USA

In a colloidal suspension containing particles of two different sizes, there is an attractive force between the larger particles. This attraction is due to the extra volume that becomes available to the smaller particles when the larger particles approach one another, thus increasing the entropy of the system. Entropic 'excluded-volume' effects of this type have been studied previously in colloids and emulsions, in the context of phase-separation phenomena in the bulk[1–15] and at flat surfaces[2,16]. Here we show how similar effects can be used to position the larger particles of a binary mixture on a substrate, or to move them in a predetermined way. Our experiments demonstrate the entropically driven repulsion of a colloidal sphere (in a suspension of smaller spheres) from the edge of a step; the magnitude of the entropic barrier felt by the sphere is approximately twice its mean thermal energy. These results indicate that passive structures etched into the walls of a container create localized entropic force fields which can trap, repel or induce the controlled drift of particles. Manipulation techniques based on these effects should be useful for making the highly ordered particle arrays required for structures with photonic band gaps[17,18], microelectronic mask materials[19], and materials for clinical assays[20].

To demonstrate the entropic force-field idea in its barest form, we investigated the motions of hard spheres near the edge of a terrace (Fig. 1). We used an aqueous suspension of spherical polystyrene particles (Seradyn, Inc., Indianapolis) with diameters 0.460 μm and 0.083 μm and volume fractions 10^{-5} and 0.30, respectively. NaCl (0.01 M) was added to screen the electrostatic interactions over a distance of ~5 nm to obtain nearly ideal hard-core interactions[16]. As discussed below, the small spheres induce a 'depletion' attraction between the large spheres and the flat surface. Thus, a large sphere placed on the terrace diffused on its surface for several seconds (before escaping to the bulk). By following the two-dimensional trajectories of these spheres, we measured the forces acting on them near the step edge.

We quantify the effect of the step edge by measuring directly the Helmholtz free energy, F, of the system as a function of the position of the large sphere (Fig. 2*a*); we follow the analytical procedure given in ref. 21. Using video microscopy, we deter-